Priority Report

Cancer Research

Oral Interleukin-10 Alleviates Polyposis via Neutralization of Pathogenic T-Regulatory Cells

Allen Y. Chung[1], Qingsheng Li[1], Sarah J. Blair[1], Magdia De Jesus[2], Kristen L. Dennis[3], Charles LeVea[4], Jin Yao[1,5], Yijun Sun[1], Thomas F. Conway[1], Lauren P. Virtuoso[1], Nicholas G. Battaglia[1], Stacia Furtado[6], Edith Mathiowitz[6], Nicholas J. Mantis[2], Khashayarsha Khazaie[3], and Nejat K. Egilmez[1]

Abstract

Immune dysregulation drives the pathogenesis of chronic inflammatory, autoimmune, and dysplastic disorders. While often intended to address localized pathology, most immune modulatory therapies are administered systemically and carry inherent risk of multiorgan toxicities. Here, we demonstrate, in a murine model of spontaneous gastrointestinal polyposis, that site-specific uptake of orally administered IL10 microparticles ameliorates local and systemic disease to enhance survival. Mechanistic investigations showed that the therapeutic benefit of this treatment derived from neutralization of disease-promoting $FoxP3^{+}RoR\gamma t^{+}IL17^{+}$ pathogenic T-regulatory cells (pgTreg), with a concomitant restoration of $FoxP3^{+}RoR\gamma t^{-}IL17^{-}$ conventional T-regulatory cells (Treg). These findings provide a proof-of-principle for the ability of an oral biologic to restore immune homeostasis at the intestinal surface. Furthermore, they implicate local manipulation of IL10 as a tractable therapeutic strategy to address the inflammatory sequelae associated with mucosal premalignancy. *Cancer Res; 74(19); 5377–85. ©2014 AACR.*

Introduction

IL10 is critical for maintenance of immune homeostasis, particularly at the gastrointestinal interface (1). In both humans and mice, IL10 deficiency is linked to the development of a wide range of immune-mediated pathologies (2, 3), including cancer (4).

Preclinical studies in murine models of inflammatory disease have demonstrated therapeutic utility for recombinant IL10 (5, 6). In clinical trials, however, intravenous administration of IL10 to patients with inflammatory bowel disease (IBD) resulted in dose-dependent paradoxical effects with only nominal therapeutic benefit (7). Because of the lack of methods for administering IL10 in a tissue-specific manner, the clinical potential of IL10 as a biologic therapeutic remains undetermined.

Previous studies have revealed that bioerodible sustained-release microparticles prepared via phase inversion nanoencapsulation (PIN) can be used for oral delivery of biologic molecules to the intestine (8). When applied to models of intestinal inflammation and dysplasia, this strategy affords the ability to target physiologic quantities of protein to the disease microenvironment with minimal escape into circulation. Although the utility of PIN for delivery of nucleic acids and peptides to the gut mucosa has been established, its effectiveness in targeting bioactive protein therapeutics to gut-associated lymphoid tissue and mesenteric lymph nodes (MLN) remains undefined.

On the basis of the previous findings that adoptive transfer of $CD4^{+}CD25^{+}$ T cells suppresses intestinal disease in the $APC^{min/+}$ mouse model of spontaneous gastrointestinal polyposis in an IL10-dependent manner (9), we sought to determine whether IL10-encapsulated PIN microparticles could directly modify the intestinal inflammatory landscape and alter the natural history of this genetically driven preneoplastic disease. The results provide the first evidence for the therapeutic potential of an oral particulate cytokine formulation, in this case IL10, to ameliorate both local and systemic disease. Furthermore, our findings identify pathogenic T-regulatory cells (pgTreg) as a primary therapeutic target of IL10 in the dysplastic intestine.

Materials and Methods

Animals

C57BL/6 (B6), B6.SJL-$Ptprc^{a}Pepc^{b}$/BoyJ (CD45.1), $APC^{min/+}$, DEREG, and $RAG1^{-/-}$ mice were purchased from Jackson

[1]Department of Microbiology and Immunology, School of Medicine and Biomedical Sciences, University at Buffalo, Buffalo, New York. [2]Division of Infectious Diseases, Wadsworth Center, Albany, New York. [3]Division of Gastroenterology, Northwestern University Feinberg School of Medicine, Chicago, Illinois. [4]Department of Surgical Pathology, Roswell Park Cancer Institute, Buffalo, New York. [5]Department of Electrical and Computer Engineering, University of Florida, Gainesville, Florida. [6]Department of Molecular Pharmacology, Physiology & Biotechnology, Brown University, Providence, Rhode Island.

Note: Supplementary data for this article are available at Cancer Research Online (http://cancerres.aacrjournals.org/).

Current address for K. Khazaie: Department of Immunology, Mayo Clinic College of Medicine, Rochester, MN 55905; and current address for Q. Li and N.K. Egilmez: Department of Microbiology and Immunology, University of Louisville School of Medicine, Louisville, KY 40202.

Corresponding Author: Nejat K. Egilmez, University of Louisville, 505 S.Hancock St., Louisville, KY 40202. Phone: 502-852-3539; Fax: 502-852-7531; E-mail: nejat.egilmez@louisville.edu

doi: 10.1158/0008-5472.CAN-14-0918

Laboratory. BALB/c mice were purchased from Taconic. $APC^{min/+}$-DEREG mice were created in house. All experiments were conducted in accordance with guidelines set forth by the Institutional Animal Care and Use Committees at the University at Buffalo (Buffalo, NY) and Wadsworth Center (Albany, NY).

Microparticle preparation and oral delivery

IL10-loaded PIN particles were prepared using a modified PIN process (10). Two formulations were produced: (i) control (no cytokine) and (ii) recombinant murine IL10 (Peprotech, Inc., >98% purity, <1 EU/μg) with a loading of 0.5 μg cytokine/mg of particles. Control or IL10 microparticles were provided by oral gavage (1 mg particles in 0.3 mL sterile water) three times per week for 4 weeks starting at 10 weeks of age. For experiments utilizing FITC-BSA microparticles, single 30 mg bolus doses were given.

Antibodies

The following antibodies were used for immunofluorescence and IHC: CD45R/B220 (RA3-6B2, BD Pharmingen), CD11c (N418, eBioscience), Fc receptor block; anti-CD16/CD32 (2.4G2, BD Pharmingen), CD3 (F7.2.38, Agilent Technologies), and von Willebrand factor (vWF; A0082, Dako). The following antibodies were used for flow cytometry: CD45.1 (A20, eBioscience), CD4 (RM4-5, eBioscience), IL17A (TC11-18H10, BD Pharmingen), FoxP3 (FJK-16s, eBioscience), RoRγt (Q31-378, BD Pharmingen), CD44 (IM7, eBioscience), IFNγ (XMG1.2, BD Pharmingen), CD8α (53-6.7, eBioscience), and γδ-TCR (eBioGL3, eBioscience). Anti-mCD4 (GK1.5, BioXCell) was used for *in vivo* $CD4^+$ T-cell depletion.

Immunofluorescence tissue collection and staining

Tissues were embedded in OCT compound (Sakura Finetek) and snap frozen in liquid nitrogen. Of note, 20-μm serial cryosections were immunostained as indicated previously (11). Scanning laser confocal images were collected using a Leica SP5 ABOS microscope and processed using Fiji Software (http://fiji.sc/).

Gross intestinal preparation and polyp quantification

Formalin-fixed intestines were opened longitudinally and polyp burdens were quantified using a dissecting microscope.

Flow cytometry

Spleens and MLN were processed into single cell suspensions. Intestines were digested and fractionated into lamina propria mononuclear cells (LPMC) and intraepithelial lymphocytes, as described previously (12). For experiments requiring detection of intracellular antigens (FoxP3, RoRγt, IL17A, and IFNγ), cell suspensions were cultured for 5 hours in the presence of Golgistop (5 μL/mL; BD), phorbol myristate acetate (50 ng/mL; Sigma), and ionomycin (1 μg/mL Sigma). Cells were then permeabilized and fixed using an intracellular staining kit (eBioscience) overnight at 4°C.

Histologic and IHC preparation

Paraffin-embedded tissue sections (5 μm) were stained with hematoxylin and eosin. For IHC, slides were subjected to antigen retrieval before application of the indicated primary antibodies. Biotinylated secondary antibodies (anti-rat IgG, BD Pharmingen), HRP-SA conjugate (Invitrogen), and diaminobenzidine chromogen (Dako) were used for visualization. Images were taken at ×400 magnification.

Histologic scoring

For intestines, histologic scores were assigned in a blinded fashion using criteria established in our laboratory (see Supplementary Data). For spleens, histologic scores were assigned using modified criteria from a previously published report (see Supplementary Data; ref. 13).

Hematologic indices

Red blood cell (RBC), hemoglobin (HgB), and hematocrit (HCT) levels were determined using a Vetscan HM5 automated analyzer (Abaxis Veterinary Diagnostics).

Mortality tracking

Mortality criteria for $APC^{min/+}$ mice were developed and applied to survival studies. A combined scoring system, taking into account the degree of weight loss and the severity of change in activity was selected (see Supplementary Data).

Microarray data processing

RNA was isolated from nonpolyp (for WT and $APC^{min/+}$ mice) and polyp sections (for $APC^{min/+}$ mice) of terminal ileum using the RNeasy Mini Kit (Qiagen) and subjected to gene expression profiling. Briefly, RNA was processed into cRNA using the Affymetrix Genechip 3′ IVT Expression Protocol and applied to Affymetrix Mouse Genome 430A 2.0 arrays. Interference from bacterial RNA was selected against using a probeset enriched in oligos extending into 3′-poly-A tails. Details with respect to sample processing and preparation can be accessed from the Gene Expression Omnibus (NIH) under accession number GSE49970.

Subtotal Treg depletion

DEREG or $APC^{min/+}$-DEREG mice received 1 μg of Diphtheria toxin (DT, Sigma) dissolved in 100 μL of Dulbecco PBS by intraperitoneal injection on days 0, 1, and 14.

In vivo Treg suppression assay

MLN $CD45.2^+CD4^+CD25^+$ cells and total lymph node $CD45.1^+CD4^+CD25^-$ cells were isolated by magnetic selection from either $APC^{min/+}$ or BoyJ mice, respectively. A total of 1×10^6 $CD45.1^+CD4^+CD25^-$ cells were CFSE labeled using the Vybrant CFDA SE cell tracer kit and adoptively transferred with 4×10^5 MLN $CD45.2^+CD4^+CD25^+$ as indicated, into 8-week-old female $RAG1^{-/-}$ recipients.

In vivo adoptive cell transfer

A total of 1×10^6 magnetically selected MLN $CD4^+CD25^+$ T cells from 14-week-old $APC^{min/+}$ mice were adoptively transferred into sex-matched 10 week old $APC^{min/+}$ recipients. Four days before transfer, recipient mice were transiently depleted of their $CD4^+$ cells using a single 300 μg i.p. dose of anti-CD4 antibody.

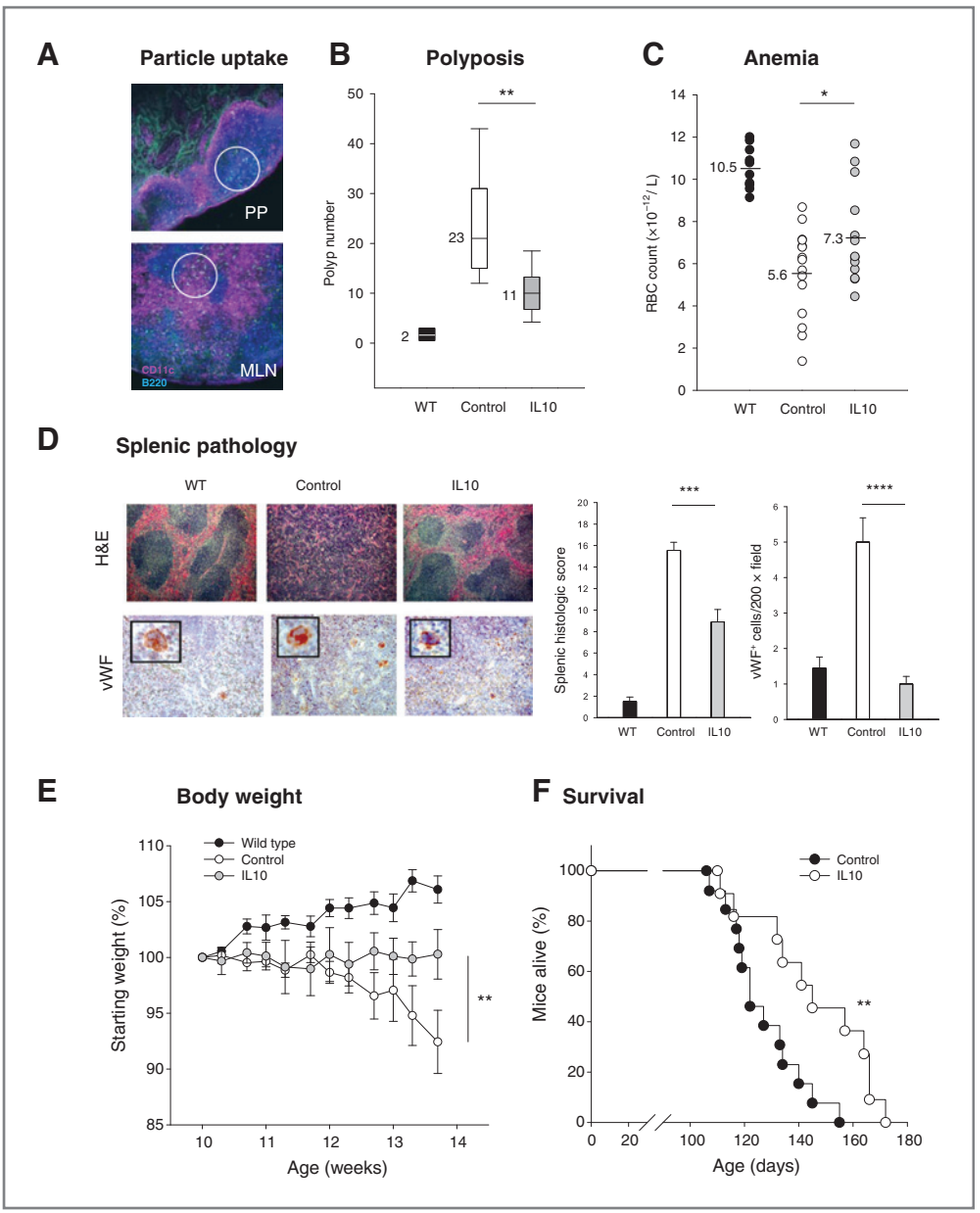

Figure 1. Chronic oral IL10 microparticle therapy alleviates polyposis and systemic disease symptoms. A, particle uptake. Six hours after oral gavage, FITC-BSA microparticles (areas circled) were localized from the Peyer's patches (PP) and MLNs of treated $APC^{min/+}$ mice. B-cells (blue, anti-B220), dendritic cells (magenta, anti-CD11c), and microparticles (green) were visualized. B, effect of treatment on polyp burden. Mice were gavaged with 1 mg of control or IL10 microspheres. Numbers indicate the mean. Boxes have lines at the median plus lower and upper quartiles, with whiskers extending to show the remaining data ($n = 5, 9, 9$, for wt, control, IL10, respectively). Increasing the IL10 dose did not improve therapeutic efficacy (data not shown). C, anemia. RBC levels ($n = 10, 15, 13$ for wt, control, IL10, respectively). D, splenic pathology. Representative H&E and anti-vWF–stained sections are shown. Megakaryocytes were visualized directly (inset). Splenic pathology scores (n is identical to A) and megakaryocytosis (over 10–12 high power fields, $n = 3$ per group) were quantified. E, body weight. Statistical comparison is made between control and IL10-treated groups ($n = 4, 6, 6$ for wt, control, IL10, respectively). F, survival. Mortality was determined for $APC^{min/+}$ mice receiving either no treatment (control) or chronic IL10 microsphere treatment ($n = 13$ and 11, respectively). Therapy was initiated on day 70. *, $P < 0.05$; **, $P < 0.01$; ***, $P < 0.001$; ****, $P < 0.0001$. Error bars, SEM.

qRT-PCR

Steady-state mRNA levels were detected with SYBR Green PCR Master Mix (Applied Biosystems) using the Mx3000p qPCR system (Agilent Technologies). Results were normalized to the expression of β-actin. The expression level was scaled using the $2^{-\Delta\Delta Ct}$ method with the average levels obtained for wild-type intestines set arbitrarily to 1. Primer sequences utilized were: β-actin forward 5′-TCACCCACACTGGCCCATC-TACGA-3′, reverse 5′-TGGTGAAGCTGTAGCCACGCT-3′; IL1β forward 5′- GCCCATCCTCTGTGACTCAT-3′, reverse 5′-AGG-CCACAGGTATTTTGTCG-3′; IL6 forward 5′-CCATCCAGTTG-CCTTCTTGG-3′, reverse 5′-TTTCTGCAAGTGCATCATCG-3′;

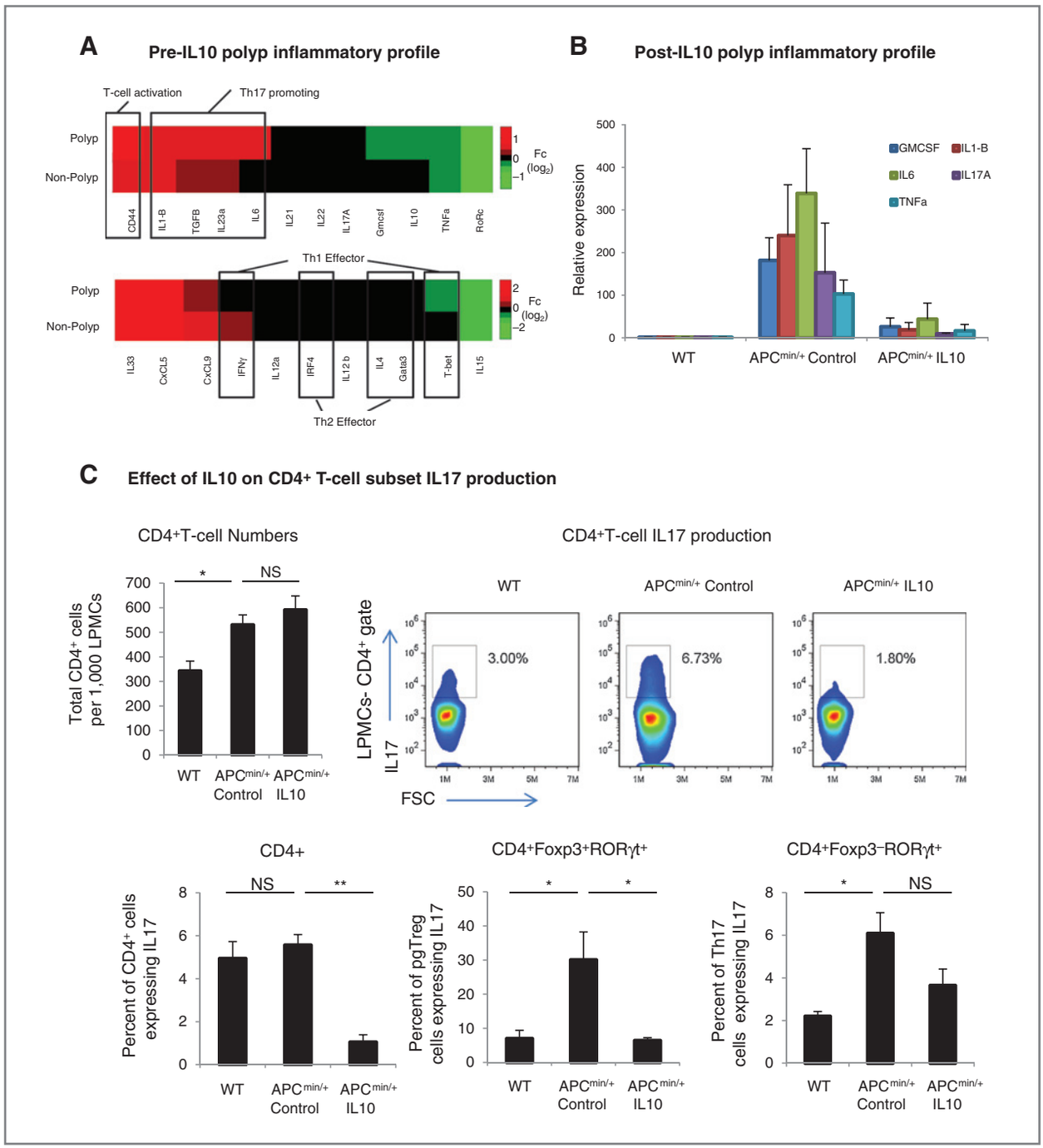

Figure 2. IL10-mediated neutralization of Th17-like intestinal inflammatory profile is associated with suppression of pgTreg IL17 production. A, pretherapy inflammatory landscape. Heatmap assessment of select T-cell related functional genes between 12-week-old APC$^{min/+}$ nonpolyp and polyp intestine ranked by average fold-change over WT nonpolyp conditions. B, posttherapy inflammatory landscape. Messenger RNA expression levels for Th17-associated cytokines from 14-week-old control or IL10 microparticle-treated mice. C, posttherapy T-cell IL17 production. LPMCs from 14-week-old control or IL10 microparticle-treated mice were analyzed ($n = 4$–6 per group). *, $P < 0.05$; **, $P < 0.01$. Error bars, SEM.

IL17A forward 5′-CTGAGCTTCCCAGATCACAGAG-3′, reverse 5′-CGCAAAAGTGAGCTCCAGAAAG-3′; GM-CSF forward 5′-CACGTTGAATGAAGAGGTAGAAG-3′, reverse 5′-CATGTTCAAGGCGCCCTTGAG-3′; TNFα forward 5′-GAACTGGCAGAAGAGGCACT-3′, reverse 5′-AGGGTCTGGGCCATAGAACT-3′.

Statistical analysis

Statistical calculations were performed using Student *t* test in pairwise comparisons of groups. Log-rank tests were utilized for survival studies. *P* values of 0.05 or less were considered statistically significant.

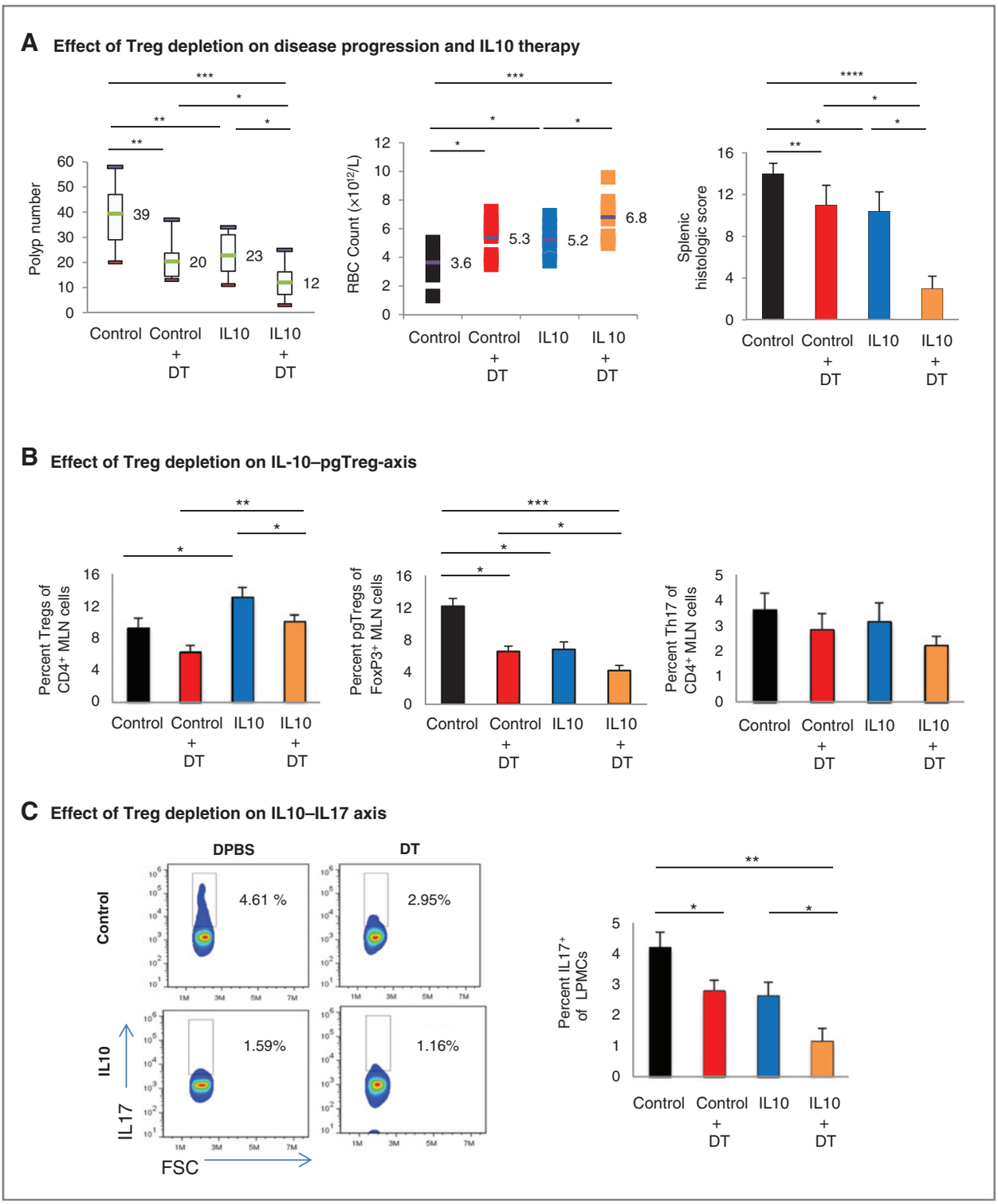

Figure 3. Subtotal depletion of Tregs in APC$^{min/+}$ mice ameliorates disease and boosts oral IL10 microparticle therapeutic effect. Ten-week-old APC$^{min/+}$-DEREG mice received either mock (PBS) or subtotal Treg depletion (DT), concomitant with either control or IL10 microparticle therapy. Disease markers were quantified at the end of the therapeutic period. A, polyp burdens, RBC levels, and splenic pathology scores. B, MLN Tregs, pgTregs, and Th17 cells. Cells were defined within the CD4$^+$ population as FoxP3$^+$RoRγt$^-$ (Treg) and FoxP3$^-$RoRγt$^+$ (Th17) or within the FoxP3$^+$ population as RoRγt$^+$ (pgTregs). C, LPMC IL17 expression profiles. Plots are representative of experimental groups and display events within a size-excluded subgate. For A and B, $n = 7$–8. For C, $n = 3$–4. *, $P < 0.05$; **, $P < 0.01$; ***, $P < 0.001$; ****, $P < 0.0001$. Error bars, SEM.

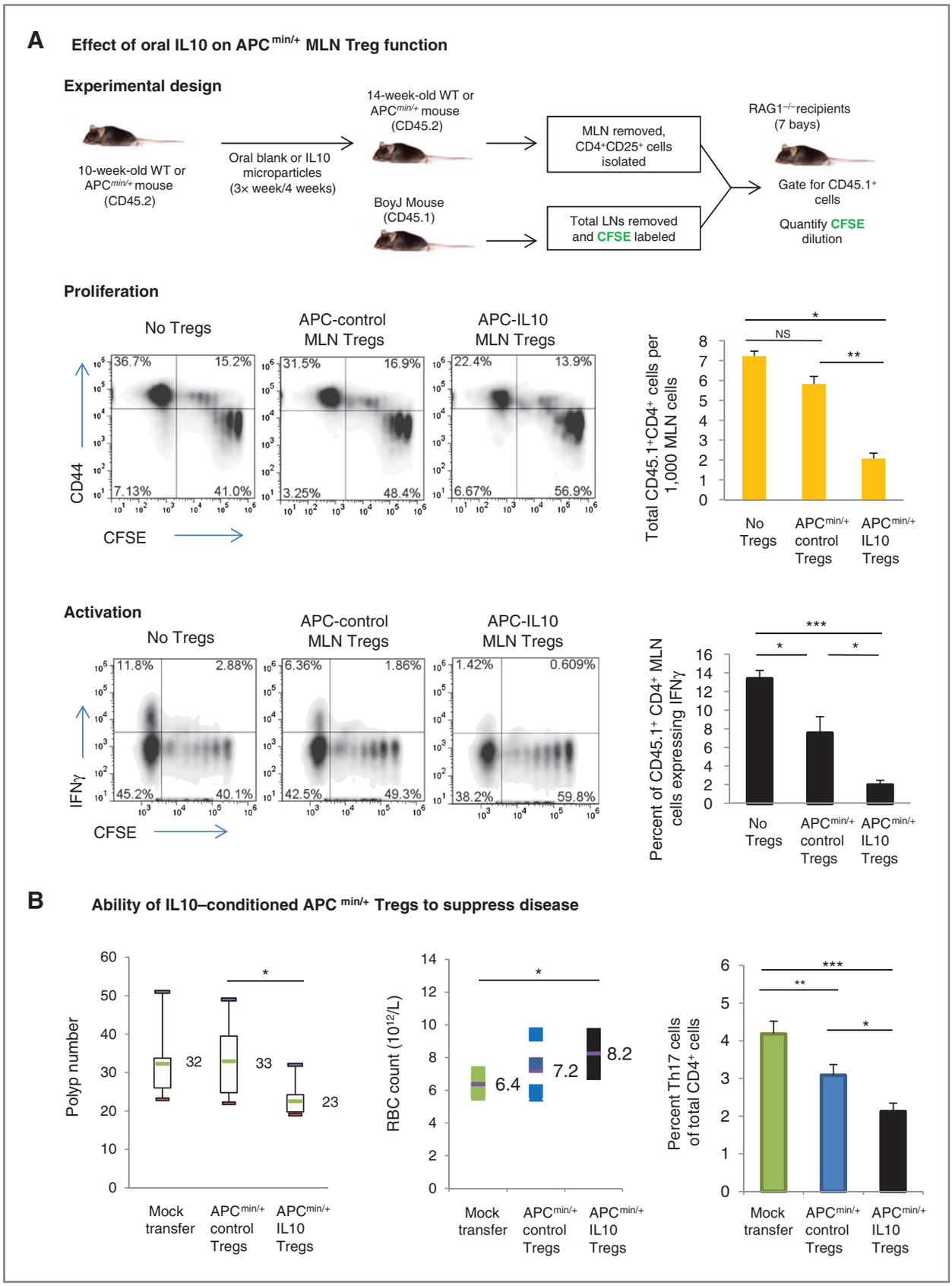

Results and Discussion

Oral PIN microparticles loaded with FITC-BSA were taken up and retained in the Peyer's patches and MLNs of both $APC^{min/+}$ and wild-type mice (Fig. 1A and Supplementary Fig. S1A and S1B). Microparticles were not detected in the colon, liver, or spleen at any time point after feeding (Supplementary Fig. S1C). Moreover, when IL10-loaded microparticles were delivered in bolus doses, IL10 could not be detected in serum (data not shown). These results suggest that uptake of microparticles and release of IL10 were effectively localized to intestinal immune structures.

We directly tested whether oral administration of IL10 microparticles could suppress established polyposis in $APC^{min/+}$ mice. Therapy resulted in a more than 2-fold reduction in polyp burden (Fig. 1B) and a decreased severity of disease pathology in the intestine (Supplementary Fig. S2A and S2B). In $APC^{min/+}$ mice, intestinal disease is accompanied by predictable systemic abnormalities, namely anemia, splenomegaly, and weight loss (14). To determine whether amelioration of local disease would result in improvement of systemic symptoms, we monitored experimental animals over the course of therapy. In all cases, treatment with IL10 resulted in significant benefit (Fig. 1C–E and Supplementary Fig. S2C). Relief of systemic symptoms was likely secondary to the suppression of chronic intestinal inflammation, as such activity has been shown to cause anemia (15) and to promote the establishment of extramedullary hematopoiesis (16). Accordingly, analysis of $APC^{min/+}$ mouse spleens revealed significant megakaryocytosis, which was abrogated following treatment (Fig. 1D). Chronic treatment resulted in a 15% extension of both median and maximal lifespan, suggesting that IL10 could suppress but not arrest disease (Fig. 1F and Supplementary Fig. S3A).

We sought to define the potential mechanisms underlying the therapeutic activity of oral IL10. Because IL17 has recently been implicated as an essential driver of polyp growth in $APC^{min/+}$ mice (17), and IL10 has been shown to suppress IL17 production by T cells (18), we hypothesized that the observed therapeutic effects of IL10 microparticles may partially be attributed to modification of T-cell activity. $APC^{min/+}$ nonpolyp and polyp areas demonstrated increasing levels of T-cell activation, with a progressive shift from a balanced T-helper (Th) 1/2/17 profile to an IL1β/IL6/IL23-enriched Th17-promoting profile during early-stage disease (Fig. 2A). Importantly, quantification of select Th17-related inducer/effector cytokines confirmed that IL10 microparticles were highly effective at suppressing the expression of these genes in mice with established disease (Fig. 2B). In contrast, treatment did not result in significant changes in IFNγ or IL4 levels (data not shown). Taken together, these results demonstrate that IL10 microparticle therapy strongly antagonizes IL17-mediated inflammation.

T cells are thought to be the primary producers of IL17 during chronic intestinal inflammation (19). Accordingly, we examined the IL17 expression profile in various types of intestinal T cells from our $APC^{min/+}$ mice. Although intraepithelial γδ-T cells did not produce significant levels of IL17 during disease (Supplementary Fig. S3B), there was an increase in both the total number of $CD4^+$ T cells and in their ability to produce IL17 (Fig. 2C). IL10 treatment did not impact the absolute numbers of $CD4^+$ T cells, but did act to dramatically reduce the percentage of IL17-producing cells within this population (Fig. 2C). Because both $FoxP3^-ROR\gamma t^+IL17^+$ Th17 cells and $FoxP3^+RoR\gamma t^+IL17^+$ pgTregs are known to be a major contributor to polyposis in this model (19–21), we examined the impact of IL10 on IL17 expression by these two subsets. IL10 treatment resulted in a dramatic reduction in IL17 production by pgTregs, with only a modest decline in IL17 production by Th17 cells (Fig. 2C). Collectively, these results suggest that of the IL17-producing T-cell subtypes present during disease, pgTregs are uniquely sensitive to modulation by IL10.

Next we examined whether modulation of pgTregs was the primary mechanism underlying IL10 microparticle therapeutic effect. We crossed $APC^{min/+}$ mice with the DEREG murine model of inducible Treg depletion and developed a subtotal Treg depletion protocol appropriate for our desire to assess the contribution of the IL10–pgTreg axis to our model system. Subtotal Treg depletion resulted in a more than 70% reduction in $FoxP3^+$ cells over 28 days, yet avoided the catastrophic myelo- and lympho-proliferative disorder typically seen in mice undergoing total Treg ablation (Supplementary Fig. S4 and S5A; ref. 22). Subtotal Treg depletion reduced polyp burden, anemia, and splenic pathology (Fig. 3A and Supplementary Fig. S5B and S5C), supporting the notion that pgTregs are the major contributors to both local and systemic disease. Administration of IL10 microparticles further enhanced depletion-induced therapeutic benefits, suggesting that IL10 was acting, in part, through neutralization of residual pgTregs. Consistent with this hypothesis, analysis of MLNs revealed that subtotal Treg depletion reduced the prevalence of pgTregs, whereas IL10 both diminished the pgTreg presence and promoted an increase in conventional Tregs; MLN Th17 cell numbers, however, remained unaffected (Fig. 3B and Supplementary Fig. S5D and S5E). Analysis of the LPMCs revealed a similar pattern, that is, both subtotal Treg depletion and IL10 therapy diminished the proportion of IL17-positive cells, but the most significant reduction was obtained in the combination treatment group (Fig. 3C). Whether the superior effect that

Figure 4. IL10-mediated neutralization of pgTregs enhances Treg-mediated suppression of polyposis. A, suppression of cellular proliferation and activation. Isolated $CD45.2^+CD4^+CD25^+$ Tregs were mixed with CFSE-labeled $CD45.1^+$ responder cells and applied to an *in vivo* Treg suppression assay. Responder cells were assessed for generation count, expression of CD44, and total number. The prevalences of $IFN\gamma^+CD45.1^+$ $CD4^+$ cells in recipient lymph nodes were also determined. B, suppression of disease. MLN $CD45.2^+CD4^+CD25^+$ cells were adoptively transferred into 10-week-old untreated $CD45.2^+$ $APC^{min/+}$ mice. Polyp burdens, RBC levels, and prevalences of MLN Th17 cells were assessed in recipients 4 weeks after transfer. For A, plots are representative of each experimental group ($n = 4$–5); for B, $n = 4$ for the Mock Transfer group and $n = 8$ for each of the transfer groups. *, $P < 0.05$; **, $P < 0.01$; ***, $P < 0.001$. Error bars, SEM.

was obtained in this group was due to the appearance of a qualitatively unique Treg population is currently under investigation.

To determine whether the dual activity of IL10 on pgTregs and Tregs resulted in altered functional capacity within the total Treg population, we tested the ability of posttherapy MLN $CD4^+CD25^+$ T cells to suppress naïve T-cell proliferation and activation. In comparison with cells isolated from control-treated $APC^{min/+}$ mice, the cells from IL10-treated $APC^{min/+}$ mice were significantly more effective at suppressing these processes both *in vivo* and *in vitro* (Fig. 4A and Supplementary Fig. S6C).

The above results demonstrated that the suppressive capacity of $APC^{min/+}$ MLN $CD4^+CD25^+$ T cells was restored by IL10 microparticle therapy. We predicted that functional rescue of $APC^{min/+}$ intestinal Treg population via reversal of the pgTreg/Treg ratio was ultimately responsible for disease amelioration. To confirm this notion, we adoptively transferred MLN $CD4^+CD25^+$ T cells from control or IL10-treated $APC^{min/+}$ mice into 10-week-old $APC^{min/+}$ recipients. IL10-conditioned $CD4^+CD25^+$ T cells reduced polyposis, corrected anemia, and decreased the prevalence of Th17 cells in recipient MLNs (Fig. 4B and Supplementary Fig. S7A–S7C). Splenic disease, however, was not alleviated after transfer (Supplementary Fig. S7D and S7E). Whether the inability to restore full therapeutic effect was due to the limitations of the experimental approach, that is, accumulation/persistence of transferred cells in the intestine, or to the absence of Treg-independent effects of IL10 microparticle therapy, that is, impacts on the innate immune system, was not determined.

Our findings demonstrate that tissue-specific delivery of a particulate cytokine formulation can change the natural history of a highly penetrant genetic condition. We propose that tissue-localized IL10 serves as a molecular rheostat, specifically modulating pgTreg function during intestinal inflammatory and dysplastic disease. The overall concepts tested here are expected to extend to other inflammation-driven diseases, especially those manifesting at mucosal surfaces, including IBD, asthma, and genital tract infection.

Disclosure of Potential Conflicts of Interest

N.K. Egilmez is the vice-president of and has ownership interest (including patents) in TherapyX, Inc. No potential conflicts of interest were disclosed by the other authors.

Authors' Contributions

Conception and design: A.Y. Chung, K. Khazaie, N.K. Egilmez
Development of methodology: A.Y. Chung, Q. Li, C. LeVea, K. Khazaie
Acquisition of data (provided animals, acquired and managed patients, provided facilities, etc.): A.Y. Chung, S.J. Blair, M. De Jesus, K.L. Dennis, C. LeVea, L.P. Virtuoso, N.G. Battaglia, S. Furtado, E. Mathiowitz, N.J. Mantis
Analysis and interpretation of data (e.g., statistical analysis, biostatistics, computational analysis): A.Y. Chung, Q. Li, S.J. Blair, K.L. Dennis, J. Yao, Y. Sun, E. Mathiowitz, N.K. Egilmez
Writing, review, and/or revision of the manuscript: A.Y. Chung, C. LeVea, Y. Sun, N.J. Mantis, K. Khazaie, N.K. Egilmez
Administrative, technical, or material support (i.e., reporting or organizing data, constructing databases): A.Y. Chung, T.F. Conway, K. Khazaie, N.K. Egilmez
Study supervision: N.K. Egilmez

Grant Support

The work was supported by the NIH (AI092133 to N.K. Egilmez; HD061916 to N.J. Mantis; and CA160436 to K. Khazaie) and the Howard Hughes Medical Institute (M. De Jesus).

Received April 2, 2014; revised June 26, 2014; accepted July 15, 2014; published OnlineFirst September 16, 2014.

References

1. Moore KW, de Waal Malefyt R, Coffman RL, O'Garra A. Interleukin-10 and the Interleukin-10 receptor. Ann Rev Immunol 2001;19:683–765.
2. Kühn R, Löhler J, Rennick D, Rajewsky K, Müller W. Interleukin-10-deficient mice develop chronic enterocolitis. Cell 1993;75:263–74.
3. Eskdale J, McNicholl J, Wordsworth P, Jonas B, Huizinga T, Field M, et al. Interleukin-10 microsatellite polymorphisms and IL-10 locus alleles in rheumatoid arthritic susceptibility. Lancet 1998;35:1282–3.
4. Howell WM, Rose-Zerilli MJ. Interleukin-10 polymorphisms, cancer susceptibility and prognosis. Fam Cancer 2006;5:143–9.
5. Powrie F, Leach MW, Mauze S, Menon S, Caddle LB, Coffman RL. Inhibition of Th1 responses prevents inflammatory bowel disease in *scid* mice reconstituted with $CD45RB^{hi}$ CD4+ T cells. Immunity 1994;1:553–62.
6. Pennline KJ, Roque-Gaffney E, Monahan M. Recombinant human IL-10 prevents the onset of diabetes in the nonobese diabetic mouse. Clin Immunol Immunopathol 1994;71:169–75.
7. Fedorak RN, Gangl A, Elson CO, Rutgeerts P, Schreiber S, Wild G, et al. The Interleukin 10 Inflammatory Bowel Disease Cooperative Study Group. Recombinant human Interleukin 10 in the treatment of patients with mild to moderately active Crohn's disease. Gastroenterology 2000;119:1473–82.
8. Mathiowitz E, Jacob JS, Jong YS, Carino GP, Chickering DE, Chaturvedi P, et al. Biologically erodible microspheres as potential oral drug delivery systems. Nature 1997;386:410–4.
9. Erdman SE, Sohn JJ, Rao VP, Nambiar PR, Ge Z, Fox JG, et al. CD4+CD25+ regulatory lymphocytes induce regression of intestinal tumors in $Apc^{Min/+}$ mice. Cancer Res 2005;65:3998–4004.
10. Egilmez NK, Jong YS, Mathiowitz E, Bankert RB. Tumor vaccination with cytokine-encapsulated microspheres. In:Driscoll B, editor. Methods in Molecular Medicine. Totowa, NJ: Humana Press; 2003. Vol 75:687–95.
11. De Jesus M, Ahlawat S, Mantis NJ. Isolating and immunostaining lymphocytes and dendritic cells from murine Peyer's patches. J Vis Exp 2013;73:e50167.
12. Weigmann B, Tubbe I, Seidel D, Nicolaev A, Becker C, Neurath MF. Isolation and subsequent analysis of murine lamina propria mononuclear cells from colonic tissue. Nat Prot 2007;2:2307–11.
13. Miao EA, Leaf IA, Treuting PM, Mao DP, Dors M, Sarkar A, et al. Caspase-1-induced pyroptosis is an innate immune effector mechanism against intracellular bacteria. Nat Immunol 2010;11:1136–42.
14. Moser AP, Pitot HC, Dove WF. A dominant mutation that predisposes to multiple intestinal neoplasia in the mouse. Science 1990;247:322–4.
15. Means RT Jr, Krantz SB. Progress in understanding the pathogenesis of the anemia of chronic disease. Blood 1992;80:1639–47.
16. Griseri T, McKenzie BS, Schiering C, Powrie F. Dysregulated hematopoietic stem and progenitor cell activity promotes Interleukin-23-driven chronic intestinal inflammation. Immunity 2012;37:1–14.
17. Chae W-J, Gibson TF, Zelterman D, Hao L, Henegariu O, Bothwell AL. Ablation of IL-17A abrogates progression of spontaneous intestinal tumorigenesis. Proc Natl Acad Sci 2010;107:5540–4.
18. Huber S, Gagliani N, Esplugues E, O'Connor W Jr, Huber FJ, Chaudhry A , et al. Th17 cells express Interleukin-10 receptor and are controlled by $Foxp3^-$ and $Foxp3^+$ regulatory CD4+ T cells in an Interleukin-10-dependent manner. Immunity 2011;34:554–65.

19. Esplugues E, Huber S, Gagliani N, Hauser AE, Town T, Wan YY , et al. Control of T_H17 cells occurs in the small intestine. Nat Lett 2011;475:514–8.
20. Gounaris E, Blatner NR, Dennis K, Magnusson F, Gurish MF, Strom TB, et al. T-regulatory cells shift from a protective anti-inflammatory to a cancer-promoting proinflammatory phenotype in polyposis. Cancer Res 2009;69:5490–7.
21. Blatner NR, Mulcahy MF, Dennis KL, Scholtens D, Bentrem DJ, Phillips JD , et al. Expression of RORγt marks a pathogenic regulatory T cell subset in human colon cancer. Sci Transl Med 2012;4:1–11.
22. Kim J, Lahl K, Hori S, Loddenkemper C, Chaudhry A, deRoos P, et al. Cutting Edge: depletion of Foxp3$^+$ cells leads to induction of autoimmunity by specific ablation of regulatory T cells in genetically targeted mice. J Immunol 2009;183:7631–4.